

Doping effect of Pr₆O₁₁ on superconductivity and flux pinning of MgB₂ bulk

X. F. Pan¹, T. M. Shen¹, G. Li¹, C. H. Cheng², and Y. Zhao^{*1,2}

¹ Key Laboratory of Advanced Technologies of Materials (Ministry of Education of China), Superconductivity R&D Center (SRDC), Mail Stop 165#, Southwest Jiaotong University, 610031 Chengdu, Sichuan, P.R. China

² School of Materials Science and Engineering, University of New South Wales, 2052 Sydney, NSW, Australia

Received 22 October 2006, revised 21 January 2007, accepted 24 January 2007

Published online 13 March 2007

PACS 61.10.Nz, 61.72.Ww, 74.25.Ha, 74.25.Qt, 74.70.Ad

Bulk samples of MgB₂ doped with 0, 1, 3, and 5 wt% Pr₆O₁₁ nanopowder were prepared using a solid-state reaction route. The lattice constants of Pr₆O₁₁-doped MgB₂ systematically increase with increasing doping level, indicating a partial substitution of Pr for Mg in the crystal structure, and consequently, the superconducting transition temperature, T_c , of MgB₂ is slightly suppressed. At a low doping level of 1 wt% Pr₆O₁₁, the critical current density, J_c , and the irreversibility field, H_{irr} are improved. However, at higher doping levels, Pr₆O₁₁ doping seems harmful for the performance of MgB₂ in high magnetic fields. It is argued that the effect of the doping mechanism of Pr₆O₁₁ on T_c and J_c is quite different from those of other rare-earth elements, such as Y or Dy.

© 2007 WILEY-VCH Verlag GmbH & Co. KGaA, Weinheim

1 Introduction

The discovery of the MgB₂ superconductivity has generated great interest in the field of applied superconductivity because MgB₂ has a critical transition temperature T_c of 39 K [1], reaching the record T_c of noncuprate superconductors. Compared with the high-temperature superconductors (HTS), MgB₂ has simple structure, low processing cost, and does not have the weak-link problem at grain boundaries that hampers the applications of HTS-based superconductivity technologies. The advantages of MgB₂ make it a promising candidate for engineering applications in the temperature range 20–30 K, in which the traditional low-temperature superconductors (LTS) cannot play any roles.

One of the major problems of MgB₂-based superconductivity technologies is that the critical current density J_c of MgB₂ materials is still not high enough to satisfy the industrial applications, especially under high magnetic field. A rapid drop of J_c with the increase of applied magnetic field indicates a lack of effective pinning centers, such as second-phase particles, crystal defects, dislocations, and so on, in MgB₂. Thus, it is necessary to improve the pinning behavior of MgB₂ superconductor by all possible means. Chemical doping often provides an effective way to meet this requirement, for example, the flux-pinning behavior and J_c have been improved by chemical dopants, such as Zr, Ti, nanodiamond, C, SiC, Y₂O₃ [2–7]. Furthermore, magnetic-elements such as Mn, Fe, Co, Ni [8–10] have also been doped into MgB₂, but these magnetic elements often suppress the superconductivity and degrade its performance in

* Corresponding author: e-mail: yzhao@swjtu.edu.cn, Phone: +86 28 8760 0786, Fax: +86 28 8760 1824

a magnetic field due to the existence of a local magnetic field. Rare-earth elements (RE) often possess a strong magnetic moment, however, it seems that they do not suppress the superconductivity of MgB₂ [6, 11]. Recently, it is reported that Dy₂O₃-doped MgB₂ shows a significantly enhanced J_c in a low or medium field (2–4 T) [11].

The doping effects of rare-earth elements in MgB₂ have not been so intensively studied. More studies are necessary to explore the possible new approaches of improving the performance of MgB₂ by rare-earth element doping. For this purpose, the doping effect of Pr₆O₁₁ on the superconductivity and flux pinning of MgB₂ is studied in this work. The reasons that Pr₆O₁₁ is chosen as the dopant in this work include: (1) Pr often exhibits a complex valence state, different from Y₂O₃, thus Pr doping may result in some unexpected results; (2) Pr often exhibits a strong magnetic moment, thus it is helpful to investigate the effect of magnetic ions of a rare-earth element on T_c and other superconducting properties of MgB₂; (3) Pr has a strong suppression on T_c of HTS, thus it is interesting to note if such a suppression exists in the MgB₂ system.

2 Experimental

A series of Pr₆O₁₁-doped MgB₂ samples with mass ratios of MgB₂:Pr₆O₁₁ = (1 - x):x (x = 0, 0.01, 0.03, and 0.05) were prepared by solid-state reaction at ambient pressure. Mg (99%), B (amorphous, 99.9%), Pr₆O₁₁ (99.9%) nanopowder (100 nm) were mixed and pressed into cylinders with a diameter of 10 mm under a pressure of 10 MPa. Then the pressed samples were wrapped in Fe foil and sintered at 750 °C for 1 h in flowing Ar, and finally cooled to room temperature in a tube furnace. An excess of Mg powder was added simultaneously around the samples to compensate the loss of Mg due to its evaporation at high temperature. In the experiment, the MgB₂ samples with a density of 1.35 g/cm³ in undoped and approximately 1.42 g/cm³ in the doped samples have been obtained. The crystal structure was investigated by XRD (X'Pert Pro, PANalytical) with Cu K_α radiation. The magnetic property of samples were measured over a temperature range of 5–45 K using a physical properties measurement system (PPMS, Quantum Design), and the magnetization measurements were performed with a 1 mT applied field in zero-field cooling (ZFC). The magnetic J_c was calculated from the width, ΔM , of the magnetization loops ($M-H$) using the Bean model [12], $J_c = 20 \Delta M/[a'(1 - a'/3b')]$, where a' and b' are the dimensions of the sample perpendicular to the direction of the applied magnetic field with $a' < b'$. H_{irr} values were determined from the closure of the hysteresis loops with a criterion of $J_c = 10^2 \text{ A cm}^{-2}$.

3 Result and discussion

Figure 1a shows the XRD patterns of the Pr₆O₁₁-doped and undoped MgB₂ samples. Besides MgB₂ phase, small quantities of MgO and PrB₆ are indicated. There are no peaks corresponding to Mg, B or Pr₆O₁₁ observed. This is quite different from the situation in Y₂O₃-doped MgB₂ in which most of the Y₂O₃ dopant is not decomposed [6]. This result is also different from Dy₂O₃-doped MgB₂ in which the main impurity phase is DyB₄, other than DyB₆ [8], indicating that the Pr doping has a different effect on the phase structure of the doped MgB₂. The detailed XRD results show (Fig. 1b), that (100) and (002) reflections shift towards low diffraction angles for Pr₆O₁₁-doped samples. The doping-level dependence of the lattice constants for the Pr₆O₁₁-doped MgB₂ is shown in Fig. 2 from which an expansion of the a -axis and c -axis lattice parameters can be clearly seen. This indicates that Pr has partially substituted Mg, forming a (Mg,Pr)B₂ alloy. Although the lattice parameters increase with doping level, this increase soon becomes saturated, indicating a small solid solubility of Pr in MgB₂. This may be why the amount of PrB₆ increases rapidly with doping level, as shown by the rapid increase of the intensity of PrB₆ reflections in the XRD patterns shown in Fig. 1a. It is evident that the influence of Pr₆O₁₁ doping on the crystal structure of MgB₂ is quite different from that by doping with Y₂O₃ or Dy₂O₃ since Y₂O₃ or Dy₂O₃ cannot be doped into the MgB₂ lattice but only form impurity phases mixed within the MgB₂ matrix.

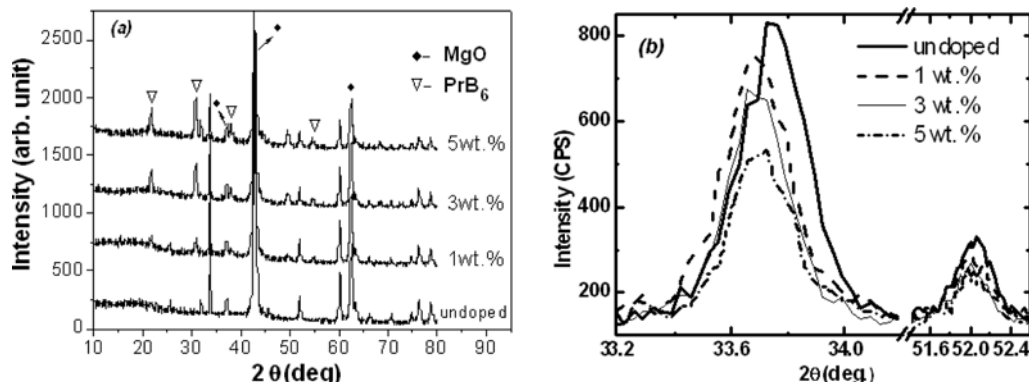


Fig. 1 (a) XRD patterns of Pr_6O_{11} -doped MgB_2 with doping levels of 0, 1, 3, and 5 wt%. (b) The [100] and [002] reflections for Pr_6O_{11} -doped and undoped MgB_2 samples, which shows that the reflection shift to lower diffraction angle with increasing doping level.

Figure 3 shows typical results of the temperature dependence of magnetization for the Pr_6O_{11} -doped MgB_2 samples. All of these samples show a sharp superconducting transition with a T_c spanning a small range of 35–38 K, indicating a good quality and uniformity of the samples. With increasing doping level, T_c is slowly but steadily depressed (see the inset of Fig. 3). This slow suppression of T_c is consistent with the slow increase of lattice parameters with doping level, and may be regarded as the consequence of the partial substitution of Pr at Mg site. It is obvious that the suppression of T_c by Pr doping is not serious because Pr doping does not directly affect the boron sheet that is believed to be responsible for superconductivity in MgB_2 . For example, compared to the undoped MgB_2 sample, the T_c of the 1 wt% Pr_6O_{11} -doped sample drops by 0.2 K. This very moderate suppression of T_c by Pr doping might suggest that the pair-breaking effect of the magnetic moment of the rare-earth element is not striking in MgB_2 . However, as reflected by the changes of T_c and the lattice parameters, Pr doping is quite different from Y or Dy doping, which have no influence on the crystal structure and T_c of MgB_2 .

The variation of J_c with applied magnetic field at 10, 20, and 30 K for the doped and undoped samples is shown in Fig. 4a. At the low doping level of 1 wt%, Pr_6O_{11} doping has clearly improved the J_c performance at all temperatures comparing with the undoped sample, although the T_c of Pr_6O_{11} -doped sample is slightly lower than that of the undoped one. For example, at 10 K, the J_c for the 1 wt% Pr_6O_{11} -doped one reaches $1.6 \times 10^5 \text{ A/cm}^2$ at 0.5 T and $4.5 \times 10^4 \text{ A/cm}^2$ at 2 T, respectively, whereas the J_c of the undoped was $1.2 \times 10^5 \text{ A/cm}^2$ at 0.5 T and $3.3 \times 10^4 \text{ A/cm}^2$ at 2 T. However, as the doping level increased, the improvement of $J_c(H)$ by Pr_6O_{11} doping is no longer pronounced. At a doping level of 3 wt%, the doped sample has a slightly higher J_c than the undoped one in the low-field region, but the J_c

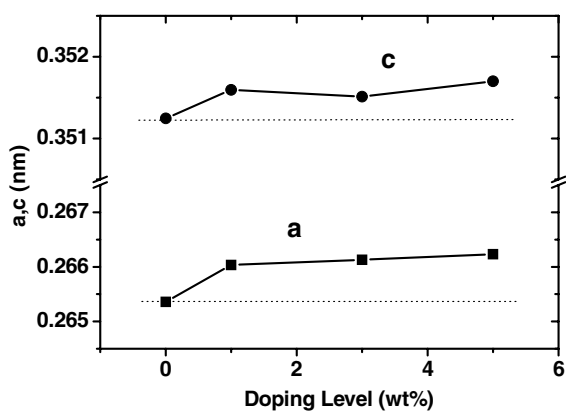


Fig. 2 Variation of the lattice parameters a and c with doping level for Pr_6O_{11} -doped MgB_2 . The solid lines are guides to the eye.

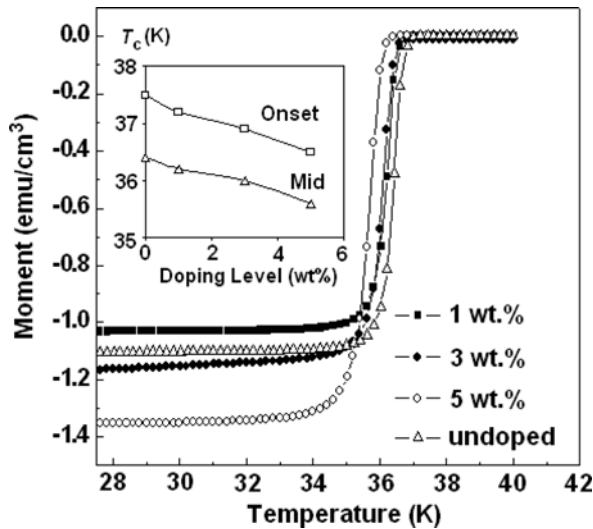


Fig. 3 Volume magnetization vs. temperature curves for Pr₆O₁₁-doped MgB₂ with doping levels of 0, 1, 3, and 5 wt%. Measurement was done in 1 mT in the ZFC process. Inset: Variation of superconducting transition temperature T_c (at onset and middle point) with doping level for Pr₆O₁₁-doped MgB₂.

in high field is lower than that of the undoped sample. At a doping level of 5 wt%, the Pr₆O₁₁-doped sample performs worse than the undoped one at all temperatures and in the whole magnetic field range in this study. The Pr₆O₁₁-doping effect on the irreversibility behavior of MgB₂ shows a similar feature as that on J_c . As can be seen in Fig. 4b that illustrates the variation of H_{irr} (10 K) with doping level, the H_{irr} (10 K) value increases at low doping level, reaches 7.2 T at the 1 wt% doping level (for comparison, the undoped one has a H_{irr} of 6.9 T at 10 K), but soon decreases with further increasing doping level. Another phenomenon worthy of note is that there is a correlation between the full width at half-maximum (FWHM) of the (100) peak in the XRD pattern with the irreversibility field for the samples studied in this work. As shown in Fig. 1b, the FWHM of the (100) peak varies with the doping level. What is interesting is that both the FWHM of the (100) peak and H_{irr} vary with doping level in a very similar way, as shown in Fig. 4b. When H_{irr} is high, the (100) peak of the corresponding sample is significantly broadened, and vice versa. Because the (100) peak of MgB₂ reflects the lattice constant of a honeycomb boron sheet in the MgB₂ structure, the broadening of this peak may suggest the occurrence of some distortion of the sheet. This result is consistent with the report of Yamamoto et al. [13] who observed that the FWHM of the (110) peak, which also corresponds to distortion of the honeycomb boron sheet in MgB₂, has a positive correlation with the H_{irr} of MgB₂, that is, H_{irr} increases with increasing FWHM of the (110) peak. Because the honeycomb boron sheet is responsible for the superconductivity in MgB₂, a distortion of the sheet may result in imperfection-induced-scattering for charge carriers, thus an enhanced H_{c2} . Therefore, the underpinning mechanism behind the correlation between FWHM of the (100) peak and H_{irr} should be the impurity-induced enhancement of H_{c2} . For the sake of comparison, the mass density, T_c , ΔT_c , H_{irr} and J_c data for samples studied in this work are summarized in Table 1.

As is well known, the behavior of J_c of a superconductor at high magnetic field is largely governed by both the flux-pinning force and the strength of upper critical field. For MgB₂, carbon doping usually

Table 1 Summary of mass density, T_c , ΔT_c , H_{irr} and J_c data for samples studied in this work.

sample	Pr ₆ O ₁₁ (wt%)	density (g/cm ³)	T_c^{mid} (K)	ΔT_c (K)	$H_{irr, 10 K}$ (T)	$J_{c, 10 K, 2 T}$ (A/cm ²)
1	0	1.35	36.4	1.9	6.9	3.0×10^4
2	1	1.42	36.2	1.8	7.2	4.5×10^4
3	3	1.40	36.0	1.8	6.6	3.3×10^4
4	5	1.40	35.6	2.1	6.5	2.1×10^4

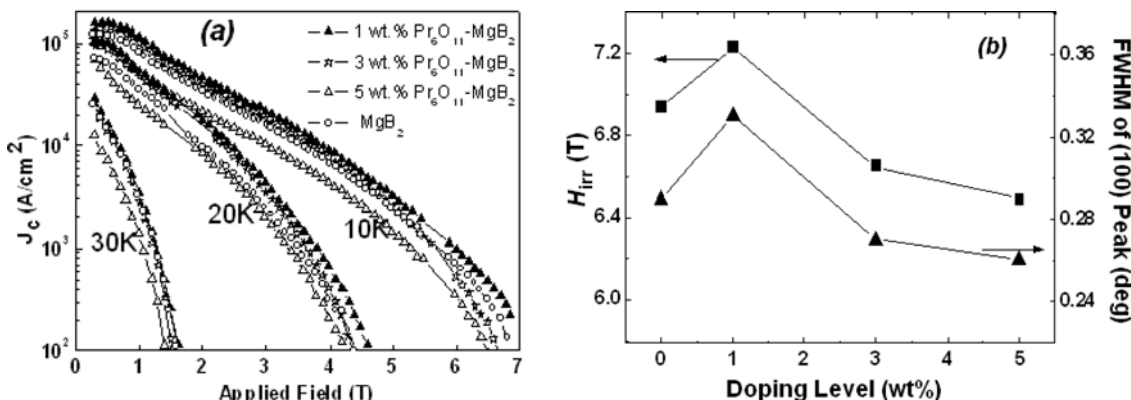


Fig. 4 (a) Magnetic-field dependence of critical current density J_c at various temperatures for Pr₆O₁₁-doped MgB₂ with various doping levels. (b) Variations of irreversibility field H_{irr} (10 K) and FWHM of (100) peak with doping level Pr₆O₁₁-doped MgB₂. A positive correlation between H_{irr} and the FWHM of the (100) peak can be clearly seen.

affects the conduction band, resulting in an enhancement of impurity scattering, and, consequently, an improvement the H_{c2} [14]. Therefore, although the T_c of MgB₂ is suppressed by carbon doping, the $J_c(H)$ behavior is largely improved, especially at high fields. In the present study, the dopant occupies the Mg site other than the boron sheet that is responsible for electron conduction and the superconductivity. Therefore, Pr doping in MgB₂ may only slightly affect the electron scattering. As a consequence, the T_c is depressed slightly, and H_{c2} may also be affected insignificantly. This may explain why the improvement of J_c and H_{irr} in Pr₆O₁₁-doped MgB₂ is not as pronounced as that in carbon-doped MgB₂. Also, different from Y₂O₃- or Dy₂O₃-doped MgB₂ [6, 11] where Y₂O₃ (or Dy₂O₃) nanoparticles serve as pinning center for magnetic flux, Pr₆O₁₁ nanoparticles has decomposed and formed PrB₆, as revealed by XRD analysis (see also Fig. 1a), thus they cannot be expected to serve as nano-pinning centers in the present system. TEM analysis (the results are not shown here) indicating that the PrB₆ is mainly segregated at grain boundary region of MgB₂, which is quite different from the microstructure of nanodiamond or Y₂O₃-doped MgB₂, where the nanoparticles are inserted in the MgB₂ matrix. Therefore, the improved flux-pinning behavior in our samples can be mainly attributed to the Pr-doping effect in Mg sites, other than the flux pinning being severed by secondary phases. In addition, the segregation of PrB₆ at grain boundaries may degrade the MgB₂ grain connection, which may be why J_c decreases with an increased amount of PrB₆ in Pr₆O₁₁-doped MgB₂.

4 Summary

In summary, Pr₆O₁₁-doped MgB₂ samples with various doping levels were prepared by solid-state reaction at ambient pressure. Pr₆O₁₁ doping affects the crystal structure of MgB₂, resulting in a systematic increase of the lattice constants with increasing doping level, thus suggesting a partial substitution of Pr for Mg in MgB₂ crystal structure. As a result, the superconducting transition temperature, T_c , of MgB₂ is slightly but steadily suppressed. At a low doping level of 1 wt% Pr₆O₁₁, the critical current density, J_c , and the irreversibility field, H_{irr} are improved. High-level doping (>3 wt%) of Pr₆O₁₁ in MgB₂ is harmful for the performance of MgB₂ in high magnetic fields due to the segregation of PrB₆ at the grain boundaries of MgB₂ grains, which degrades the grain connection.

Acknowledgements The authors are grateful to the National Science Foundation of China (grant No. 50372052, 50430137, 50588201); the Southwest Jiaotong University R&D Program (grant No. 2004A02), the Sichuan Province Government Research Funding (2004A02), and the Australian Research Council (grant No. DP0452522, DP0559872) for the financial support.

References

- [1] J. Nagamatsu, N. Nakagawa, T. Muranaka, Y. Zenitani, and J. Akimitsu, *Nature* **410**, 63 (2001).
- [2] Y. Zhao, Y. Feng, C. H. Cheng, L. Zhou, Y. Wu, T. Machi, Y. Fudamoto, N. Koshizuka, and M. Murakami, *Appl. Phys. Lett.* **79**, 1154 (2001).
- [3] Y. Zhao, D. X. Huang, Y. Feng, C. Cheng, T. Machi, N. Koshizuka, and M. Murakami, *Appl. Phys. Lett.* **80**, 1640 (2002).
- [4] Y. Zhao, C. H. Cheng, X. F. Rui, H. Zhang, P. Munroe, H. M. Zeng, N. Koshizuka, and M. Murakami, *Appl. Phys. Lett.* **83**, 2916 (2003).
- [5] T. Takenobu, T. Ito, Dam Hieu Chi, K. Prassides, and Y. Iwasa, *Phys. Rev. B* **64**, 134513 (2001).
- [6] J. Wang, Y. Bugoslavsky, A. Berenov, L. Cowey, A. D. Caplin, L. F. Cohen, L. D. Cooley, X. Song, and D. C. Larbalestier, *Appl. Phys. Lett.* **81**, 2026 (2002).
- [7] S. X. Dou, S. Soltanian, J. Horvat, X. L. Wang, S. H. Zhou, M. Ionescu, H. K. Liu, P. Munroe, and M. Tomsic, *Appl. Phys. Lett.* **81**, 3419 (2002).
- [8] M. Kuhberger and G. Gritzner, *Physica C* **370**, 39 (2002).
- [9] H. Kitaguchi and H. Kumakura, *Supercond. Sci. Technol.* **18**, S284 (2005).
- [10] C. H. Cheng, Y. Zhao, X. T. Zhu, J. Nowotny, C. C. Sorrell, T. Finlayson, H. Zhang, *Physica C* **386**, 588 (2003).
- [11] S. K. Chen, M. Wei, and J. L. MacManus-Driscoll, *Appl. Phys. Lett.* **88**, 192512 (2006).
- [12] C. P. Bean, *Rev. Mod. Phys.* **36**, 31 (1964).
- [13] A. Yamamoto, J. Shimoyama, S. Ueda, Y. Katsura, I. Iwayama, S. Horii, and K. Kishio, *Appl. Phys. Lett.* **86**, 212502 (2005).
- [14] A. Gurevich, *Phys. Rev. B* **67**, 184515 (2003).